J. Fluid Mech. (1994), *vol.* 277, *pp.* 227–248

On the direct initiation of gaseous detonations by an energy source

By LONGTING HE AND PAUL CLAVIN

Laboratoire de Recherche en Combustion, URA 1117 CNRS and Université d'Aix-Marseille I, Service 252, Centre St-Jérôme, 13397 Marseille CEDEX 20 France

(Received 12 November 1993 and in revised form 25 April 1994)

A new criterion for the direct initiation of cylindrical or spherical detonations by a localized energy source is presented. The analysis is based on nonlinear curvature effects on the detonation structure. These effects are first studied in a quasi-steady-state approximation valid for a characteristic timescale of evolution much larger than the reaction timescale. Analytical results for the square-wave model and numerical results for an Arrhenius law of the quasi-steady equations exhibit two branches of solutions with a C-shaped curve and a critical radius below which generalized Chapman–Jouguet (CJ) solutions cannot exist. For a sufficiently large activation energy this critical radius is much larger than the thickness of the planar CJ detonation front (typically 300 times larger at ordinary conditions) which is the only intrinsic lengthscale in the problem. Then, the initiation of gaseous detonations by an ideal point energy source is investigated in cylindrical and spherical geometries for a one-step irreversible reaction. Direct numerical simulations show that the upper branch of quasi-steady solutions acts as an attractor of the unsteady blast waves originating from the energy source. The critical source energy, which is associated with the critical point of the quasi-steady solutions, corresponds approximately to the boundary of the basin of attraction. For initiation energy smaller than the critical value, the detonation initiation fails, the strong detonation which is initially formed decays to a weak shock wave. A successful initiation of the detonation requires a larger energy source. Transient phenomena which are associated with the intrinsic instability of the quasi-steady detonations branch develop in the induction timescale and may induce additional mechanisms close to the critical condition. In conditions of stable or weakly unstable planar detonations, these unsteady phenomena are important only in the vicinity of the critical conditions. The criterion of initiation derived in this paper works to a good approximation and exhibits the huge numerical factor, 10^6–10^8, which has been experimentally observed in the critical value of the initiation energy.

1. Introduction

Direct initiation of gaseous detonation by an energy source is an old problem (Laffitte 1925; Zeldovich, Kogarko & Simonov 1956) which was reviewed more recently by Lee (1977, 1984). Different regimes are identified from the experiments. For a subcritical level of the total energy of the igniter $\tilde{E}_s$, $\tilde{E}_s < \tilde{E}_c$, the strong overdriven detonation wave which is first established decays rapidly, the reaction front separates completely from the shock wave, a premixed flame trails behind the shock and no detonation is initiated. With an energy larger than the critical threshold value $\tilde{E}_c$, $\tilde{E}_s > \tilde{E}_c$, the shock wave and the reaction zone remain coupled and the strong detonation originating from the source relaxes to a wave propagating at the constant

Chapman–Jouguet (CJ) velocity $\tilde{D}_{CJ}$ of the mixture. Experiments show that the onset of this CJ detonation occurs at a certain distance $\tilde{R}^*(\tilde{E}_s)$ from the point source. The order of magnitude of $\tilde{R}^*(\tilde{E}_s)$ is obtained by equating the igniter energy $\tilde{E}_s$ and the chemical energy released within the sphere bounded by the shock, to give $\tilde{E}_s \approx \tilde{\rho}_0 \tilde{Q} \tilde{R}^{*j+1}$, where $\tilde{\rho}_0$ is the density of the initial reactive mixture and $\tilde{Q}$ is the chemical heat release per unit mass, $\tilde{E}_s$ is the total energy in spherical geometry ($j = 2$) and the energy per unit length and per unit surface in cylindrical ($j = 1$) and planar geometry ($j = 0$). A critical radius is associated with the critical energy, $\tilde{R}_c = \tilde{R}^*(\tilde{E}_c)$ and no CJ detonation can be observed with a front radius $\tilde{R}_s$ smaller than $\tilde{R}_c$. Experiments show that $\tilde{R}_c$ is about ten to twenty times larger than the cell spacing size which is itself ten to fifty times larger than the thickness of the reaction zone in a planar detonation (see Desbordes 1986).

When the multi-dimensional effects are neglected, the problem is represented by a system of unsteady one-dimensional conservation equations. The rate of heat release introduces a timescale $\tilde{t}_{CJ}$ controlled by the chemical kinetics. Preliminary insight into the problem may be obtained by considering $\tilde{t}_{CJ}$ as infinitely small. Two self-similar solutions are relevant in two different time ranges of the total evolution.

(i) At early times, the total heat released by the chemical reactions is negligibly small compared to $\tilde{E}_s$, and the self-similar solution of Taylor (1950*a*) and Sedov (1946) for strong adiabatic blast waves resulting from an instantaneous deposition of energy at a point is valid

$$\tilde{E}_s = k_j[\tfrac{1}{2}(j+3)]^{j+1} \tilde{\rho}_0 \tilde{D}^{j+3} \tilde{t}^{j+1} \Leftrightarrow \tilde{E}_s = k_j \tilde{\rho}_0 \tilde{D}^2 \tilde{R}_s^{j+1}, \tag{1.1a}$$

where $\tilde{D}$ and $\tilde{R}_s$ are the velocity and the radius of the shock wave at any instant of time $\tilde{t}$ and k_j is a dimensionless constant of order unity. Different conditions are necessary for the relevance of (1.1*a*) in the detonation initiation problem: the Mach number of the leading shock must be sufficiently large; the finite element of space in which the initiation energy $\tilde{E}_s$ is deposited must be much smaller than $\tilde{R}^*(\tilde{E}_s)$; and the deposition time $\tilde{t}_s$ must be much smaller than $\tilde{t}^*(\tilde{E}_s)$ which is defined by setting $\tilde{R}_s = \tilde{R}^*$ in (1.1*a*), $\tilde{t}_s \ll \tilde{t}^*(\tilde{E}_s)$. More precisely, the self-similar law (1.1*a*) is valid for the direct initiation of detonations in the intermediate range of time,

$$\tilde{t}_s \ll \tilde{t} \ll \tilde{t}^*(\tilde{E}_s). \tag{1.1b}$$

Notice that the radius at which the non-reacting blast wave reaches the CJ velocity, as obtained from (1.1*a*) in the large-Mach-number approximation $\tilde{D}_{CJ}^2 \approx 2(\gamma^2 - 1)\tilde{Q}$, is of the same order of magnitude as $\tilde{R}^*(\tilde{E}_s)$ defined earlier as $\tilde{E}_s \approx \tilde{\rho}_0 \tilde{Q} \tilde{R}^{*j+1}$.

(ii) At sufficiently long times after a successful initiation, $\tilde{t} > \tilde{t}^*(\tilde{E}_s)$, $\tilde{E}_s$ becomes negligibly small compared to the energy released by the chemical reaction. And, in the case of a stable detonation, the solution is well approximated by the self-sustained wave of Zeldovich (1942) and Taylor (1950*a*) consisting of a smooth detonation front expanding at a constant CJ velocity followed by a self-similar rarefaction wave. The selection mechanism of the minimum wave speed $\tilde{D}_{CJ}$ is understood as follows (see Landau & Lifchitz 1989). Faster self-sustained detonations waves are associated with a subsonic flow in the reference frame of the leading shock. Thus, the shock intensity is continuously weakened (down to CJ) by the rarefaction wave which is characterized by a leading weak discontinuity travelling at sonic velocity relatively to the burned gases.

Successful direct initiations of detonations may be considered as a transition from

a self-similar solution (i) to a self-similar solution (ii) which both belong to a more general set of self-similar explosion waves associated with the deposition of variable energy at the front (Barenblatt *et al.* 1980). The numerical solutions which have been carried out to describe such a transition in the limit of an infinitely fast chemical rate ($\tilde{t}_{CJ} \to 0$), show that the onset of the CJ detonation occurs in spherical geometry at $\tilde{R}^* = (1.3\tilde{E}_s/\tilde{\rho}_0\tilde{Q})^{1/3}$ for a specific heat ratio of 1.3 (see Korobeinikov 1971) and do not exhibit any critical condition $\tilde{E}_s > \tilde{E}_c$ as observed experimentally. The existence of the critical condition results from the finite value of the reaction rate $1/\tilde{t}_{CJ}$ controlling the detonation thickness $\tilde{l}_{CJ}$, and thus cannot be described in the limit $\tilde{t}_{CJ} \to 0$.

The existing theoretical models for the critical energy are essentially phenomenological. Zeldovich *et al.* (1956) provided the first criterion: successful initiation occurs when the time necessary for the blast wave to decay to the level of the leading shock of a planar CJ detonation is larger than the chemical induction time $\tilde{t}_{CJ}$. The corresponding critical initiation energy $\tilde{E}_c$ may be estimated from (1.1 *a*) in which $\tilde{E}_s$ is replaced by $\tilde{E}_c$, $\tilde{D}$ by $\tilde{D}_{CJ}$ and $\tilde{t}$ by $\tilde{t}_{CJ}$. This criterion yields a critical radius of the same order of magnitude as the thickness of the detonation $\tilde{l}_{CJ}$, $\tilde{R}_c \sim \tilde{l}_{CJ}$, in contradiction with the experimental result $\tilde{R}_c \approx 300\tilde{l}_{CJ}$ (see Desbordes 1986). As noticed by Lee (1977), the critical energy so obtained, $\tilde{E}_c \sim \tilde{\rho}_0\tilde{D}_{CJ}^2\tilde{l}_{CJ}^3$, is smaller than the experimental data by many orders of magnitude. Other phenomenological criteria have been derived (see Lee 1984) in a similar way but by replacing $\tilde{t}_{CJ}$ by larger timescales such as those obtained from measurements of cell sizes λ or critical tube diameters. Such diameter effects have been also investigated theoretically (Zeldovich 1940; Bdzil 1980). Another criterion was also proposed based on chemical kinetics considerations (see Lee 1977). Comparisons with experiments show that the criterion based on the critical tube diameter yields the best correspondence (Lee 1984).

The purpose of the present work is to provide a theoretical analysis of this critical transition involving length- and timescales which are much larger than $\tilde{l}_{CJ}$ and $\tilde{t}_{CJ}$ characterizing the inner structure of the detonation. It will be shown that the initiation threshold of cylindrical and spherical detonations is governed by a nonlinear curvature effect of the detonation front, associated with a strong sensitivity of the reaction rate to temperature variations. The front curvature which has a tendency to decrease the gas temperature competes with the heat release rate. When the temperature sensitivity is sufficiently high, a small perturbation (here the curvature effect) is sufficient to destroy the quasi-steady structure of the reaction wave, like the extinction mechanisms of diffusion and premixed flames (see Liñan 1974; Joulin & Clavin 1976).

For ordinary mixtures, chemical kinetics introduces a minimum detonation speed $\tilde{D}^*$ below which self-ignition cannot proceed sufficiently rapidly behind the leading shock because the gas temperature is below a kinetics crossover temperature. This could be used to define detonability linits in a similar way to the flammability limits studied by He & Clavin (1993). Criteria for initiating a detonation are influenced by the proximity of these limits. We will limit our attention here to cases $\tilde{D}_{CJ} > \tilde{D}^*$.

The basic equations are presented in §2. The nonlinear curvature effects are studied in the quasi-state approximation in §3. The criterion for detonation initiation is presented in §4 where direct numerical simulations are also carried out to verify its validity. The last section is devoted to a discussion of the results.

2. The basic equations

When the molecular transport is neglected and when the chemical reaction is modelled by an exothermic irreversible one-step reaction, the unsteady and one-dimensional conservation equations are

$$\frac{\partial \rho}{\partial t}+\frac{\partial(\rho u)}{\partial r}+\frac{j}{r}(\rho u)=0, \quad \frac{\partial(\rho u)}{\partial t}+\frac{\partial(\rho u^2+p)}{\partial r}+\frac{j}{r}(\rho u^2)=0, \tag{2.1a, b}$$

$$\frac{\partial e}{\partial t}+\frac{\partial[(e+p)u]}{\partial r}+\frac{j}{r}(e+p)u=0, \quad \frac{\partial(py)}{\partial t}+\frac{\partial(\rho uy)}{\partial r}+\frac{j}{r}(\rho uy)=-\rho\omega, \tag{2.1c, d}$$

with

$$p=\rho T, \quad e=\rho\left(\frac{1}{\gamma-1}T+\tfrac{1}{2}u^2+yQ\right) \tag{2.1e, f}$$

for a polytropic gas. In these equtions p, ρ, T and e are respectively the reduced pressure, density, temperature and specific energy. These variables have been made dimensionless by reference to the preshock state labelled by subscript 0: $p=\tilde{p}/\tilde{p}_0$, $\rho=\tilde{\rho}/\tilde{\rho}_0$ $T=\tilde{T}/\tilde{T}_0$ and $e=\tilde{e}/\tilde{p}_0$. Q is the dimensionless heat release parameter $Q=\tilde{Q}/(\tilde{C}_p-\tilde{C}_v)\tilde{T}_0$, where $\tilde{C}_p$ and $\tilde{C}_v$ are the specific heats at constant pressure and at constant volume. The velocity is denoted u after non-dimensionalization through division by $\tilde{c}_0/\gamma^{1/2}$ where $\tilde{c}_0$ is the sound speed at the preshock state and γ is the specific heat ratio, $\gamma=\tilde{C}_p/\tilde{C}_v$. The non-dimensional time and space variables t and r are based on a reference time $\tilde{t}_{ref}$ associated with the induction time $\tilde{t}_{CJ}$ of the planar CJ detonation and a reference lengthscale, $\tilde{r}_{ref}\equiv\tilde{t}_{ref}\tilde{c}_0/\gamma^{1/2}$ which is typically of the same order of magnitude as the thickness of the CJ detonation front $\tilde{l}_{CJ}$. When the reaction is governed by an Arrhenius law, the reduced chemical reaction rate in (2.1d) takes the form

$$\omega=y\tilde{B}\tilde{t}_{ref}\,\mathrm{e}^{-E_a/T}, \tag{2.1g}$$

where B is the frequency factor, E_a the reduced activation energy, and y the reduced mass fraction of the limiting species. The reference timescale $\tilde{t}_{ref}$ is defined for convenience as the induction time at constant pressure:

$$\tilde{t}_{ref}\equiv\frac{1}{\tilde{B}}\frac{\gamma}{\gamma-1}\frac{T_{NCJ}}{Q}\frac{T_{NCJ}}{E_a}\mathrm{e}^{E_a/T_{NCJ}}, \tag{2.2}$$

where T_{NCJ} is the reduced temperature at the Neumann state of the planar CJ detonation. These scalings are such that the reduced induction length and induction time of the planar CJ detonation, l_{iCJ} and τ_{iCJ}, are of order unity when $E_a/T_{NCJ}\gg 1$, see (A 9a, b) in the Appendix.

In the moving frame attached to the shock, (2.1a–d) can be written as

$$\frac{\partial \rho}{\partial \tau}+\frac{\partial(\rho v)}{\partial \xi}+\frac{j}{R_s-\xi}\rho(D-v)=0, \tag{2.3a}$$

$$\frac{\partial(\rho v)}{\partial \tau}+\frac{\partial(\rho v^2+p)}{\partial \xi}+\frac{j}{R_s-\xi}\rho(D-v)v-\rho\frac{\mathrm{d}D}{\mathrm{d}\tau}=0, \tag{2.3b}$$

$$\frac{\partial h}{\partial \tau}+v\frac{\partial h}{\partial \xi}-\frac{1}{\rho}\frac{\partial p}{\partial \tau}=0, \quad \frac{\partial y}{\partial \tau}+v\frac{\partial y}{\partial \xi}=-\omega, \tag{2.3c, d}$$

with reduced space and time coordinates

$$\xi=R_s-r, \quad \tau=t \qquad R_s=\int_0^t D(t')\,\mathrm{d}t', \tag{2.4a, b}$$

where D and R_s are the velocity and the position of the shock at any instant of time t, and $v = D-u$ is the flow velocity relative to the leading shock wave. The total enthalpy is

$$h = \frac{\gamma}{\gamma-1} T + \tfrac{1}{2}v^2 + yQ. \tag{2.5}$$

3. Nonlinear curvature effect

The reference timescale which has been used in (2.1 *a–d*) is of the same order of magnitude as the induction time $\tilde{t}_{CJ}$. When the characteristic time of evolution is much longer than this reaction time, unsteady terms may be neglected in (2.3). This corresponds to the quasi-steady-state approximation. Moreover, when the curvature radius of the detonation front is much larger than the detonation thickness, $R_s \gg 1$, ξ may be neglected in the factor $(R_s-\xi)$ appearing in (2.3 *a*, *b*). This is possible whenever the relaxation toward the chemical equilibrium ($y = 0$) is sufficiently fast, as for an exponential decay of y. Then, in the framework of such multiple-scales assumptions, the governing equations for the structure of a curved detonation reduce at the leading order to the following system of first-order ordinary differential equations:

$$\frac{\mathrm{d}(\rho v)}{\mathrm{d}\xi} = -\frac{j}{R_s}\rho(D-v), \qquad \frac{\mathrm{d}(\rho v^2+p)}{\mathrm{d}\xi} = -\frac{j}{R_s}\rho(D-v)v, \tag{3.1 a, b}$$

$$\frac{\mathrm{d}h}{\mathrm{d}\xi} = 0, \qquad v\frac{\mathrm{d}y}{\mathrm{d}\xi} = -\omega, \tag{3.1 c, d}$$

where the additional curvature terms on the right-hand sides of (3.1 *a*, *b*) have to be considered as perturbations $1/R_s \ll 1$. When they are omitted, (3.1 *a–c*) reduce to the ordinary conservation system describing planar detonations. The quasi-steady approximation used in (3.1 *a–d*) is meaningful whenever the unsteady terms are smaller than the perturbative curvature effects. This point will be verified *a posteriori* and is discussed in conclusion. After elimination of p and ρ, (3.1 *a–d*) can be written in the following form, suitable for the analysis of the detonation structure in the phase space v^2–y (see Fickett & Davis 1979):

$$\frac{\mathrm{d}v}{\mathrm{d}y} = -\frac{v\psi(y,v,D)}{\omega(y,v,D)\,\phi(y,v,D)}, \tag{3.2 a}$$

with $$\psi \equiv \frac{(\gamma-1)\,Q\omega}{c^2} - \frac{j}{R_s}(D-v) \quad \text{and} \quad \phi \equiv 1-\frac{v^2}{c^2}, \tag{3.2 b}$$

where the reaction time ω defined by (2.1 *g*), the local sound speed c, and the temperature T are expressed in terms of y, v, D from the total enthalpy conservation as

$$c^2 = \gamma T = \gamma + (\gamma-1)\left[\tfrac{1}{2}(D^2-v^2) + (1-y)\,Q\right]. \tag{3.2 c}$$

3.1. *Weak curvature effects*

For clarity let us first recall briefly the well-known case $j = 0$ (or $R_s = \infty$) corresponding to the planar ZND structure of a detonation front propagating at a constant velocity in a uniform gas mixture at room temperature (see Zeldovich 1940). The forward front of the detonation wave is a non-reactive shock wave in the unburnt gas. The rise in temperature ignites the gas mixture and the reaction proceeds downstream and continues until the combustion is complete. Such a two-lengthscale structure results from the high value of the reduced activation energy yielding a reaction time much

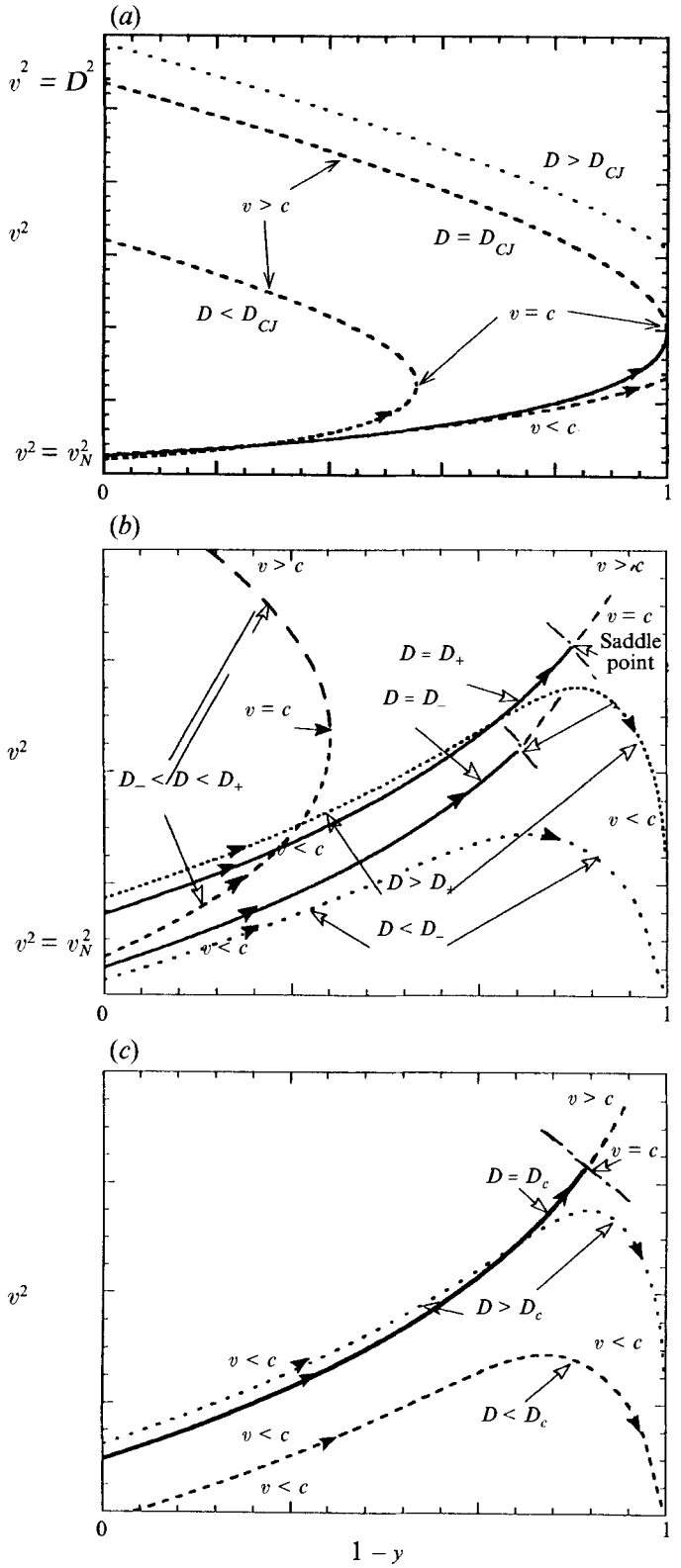

FIGURE 1. v^2–y phase diagam of quasi-steady detonation waves. (*a*) Planar detonations. (*b*) Spherical detonations for $R_s > R_c$. (*c*) Critical condition of spherical detonations, $R_s = R_c$.

larger than the elastic collision time. Thus, solutions of (3.1) or (3.2) are obtained for any given velocity D by an integration from the Neumann state, just behind the non-reactive leading shock at $\xi = 0$ ($y = 1$), to $\xi = +\infty$ where the burned mixture is assumed to be uniform (piston problem) and at equilibrium ($y = 0$). In the phase space v^2–y the problem reduces to determining the trajectories, i.e. solution of

$$\frac{\mathrm{d}v^2}{\mathrm{d}y} = -2(\gamma-1)Q\frac{v^2}{c^2(v^2,y,D)-v^2} \tag{3.2d}$$

with an initial condition $v^2 = v_N^2(D)$ at $y = 1$ given by the Hugoniot relations in the fresh gases. There is a continuum spectrum of possible velocities D which is bounded from below by the CJ case $D = D_{CJ}$. A solution exists for any value $D > D_{CJ}$ with a flow which is subsonic everywhere, $v < c$ (overdriven detonation). The marginal CJ case $D = D_{CJ}$ corresponds to a sonic velocity of the burned gases ($v_b = c_b$, $y = 0$ at $\xi = +\infty$) where, according to (3.2a, b), $\mathrm{d}v^2/\mathrm{d}y = -\infty$. There is no solution for $D < D_{CJ}$ because the trajectories turn backwards at a point corresponding to a sonic velocity $v = c$ and located before the burned gas condition: $\mathrm{d}v^2/\mathrm{d}y = -\infty$ at $0 < y < 1$ (see figure 1a). The CJ trajectory corresponds to the marginal case where the sonic point is exactly at $y = 0$. The upper branch describes a non-physical supersonic combustion process starting at $y = 1$ from the frozen preshock state. It is worthwhile to recall that in the planar case, D_{CJ} may be directly obtained by introducing the sonic condition $v_b = c_b$ at the burned gases ($y = 0$) into the integrated form of the conservation laws (3.1a–c), without solving (3.2d) which is only useful to determine the detonation structure. For a self-propagating detonation, without a moving piston in the burned gases at $v_b \leqslant c_b$, the physical mechanism of the CJ selection is, as recalled (ii) of §1, associated with the presence of a rarefaction wave in the burned gases which cannot weaken the leading shock any longer when $D = D_{CJ}$ ($v_b = c_b$).

The system of equations (3.2a–c) was used with a reaction rate ω represented by a regular function, to study the detonation structure in slightly divergent flows (Fickett & Davis 1979) or with weak curvature effects of the front (Klein & Stewart 1993). The approximate equations (3.2a, b) are valid only at the leading order of a multiple-scales analysis associated with a small parameter $1/R_s$. Only small perturbations around the planar solutions are relevant. For a given value of R_s there is a one-parameter family of solutions labelled by D. A marginal solution corresponding to a local minimum of D, called the 'generalized CJ solution' and referred to by $D_+(R_s)$ in this paper, has been found, with a sonic condition $v = c$ occurring at $y = y^* > 0$, before the completion of the reaction (see figure 5.40 of Fickett & Davis 1979). This marginal solution is qualitatively different from the CJ solution of the planar case; the condition $v = c$ corresponds to a saddle point in the phase space v^2–y ($\psi = 0$, $\phi = 0$ but $\mathrm{d}v^2/\mathrm{d}y \neq -\infty$, see the D_+ curve in figure 1b). Solutions exist for larger detonation velocities, $D > D_+$, and they all correspond to overdriven detonations with a subsonic flow ($v < c$) everywhere ($0 \leqslant y \leqslant 1$). The trajectory of the marginal solution, $D = D_+$, passes through the saddle critical point ($y = y^*$) into the supersonic region and, as a consequence, this solution is qualitatively different from all the overdriven ones; the flow is subsonic in a first part behind the shock wave, $1 \geqslant y > y^*$, and supersonic in the last part of the combustion process $y^* > y \geqslant 0$. For slightly smaller detonation velocities, $D < D_+$, the sonic condition $v = c$ corresponds to $\mathrm{d}v^2/\mathrm{d}y = -\infty$ which appears at $y > 0$ as in the planar case for $D < D_{CJ}$, and a solution no longer exists because $y = 0$ cannot be attained. The relation between D and R_s, referred below as $D(R_s)$, was obtained from the marginal solution D_+ (Klein & Stewart 1993).

The analysis presented below (see §§3.2 and 3.3) shows that there exists another branch of marginal solutions $D_-(R_s)$ ($D_- < D_+$ see figure 1b) with solutions for $D <$

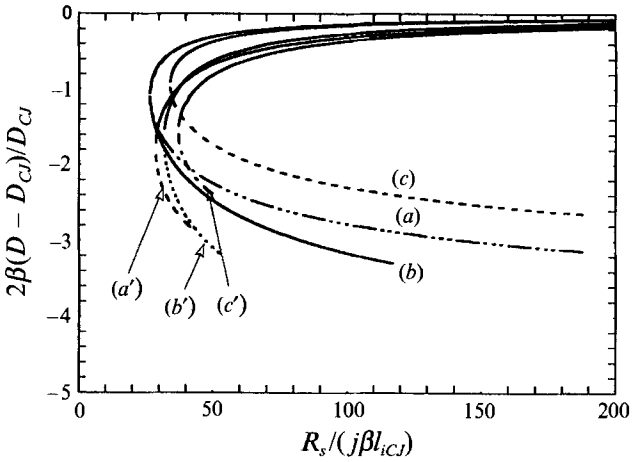

FIGURE 2. Detonation velocity as a function of the front radius for the marginal quasi-steady-state solutions. Analytical results for the square-wave model: (*a*) $\gamma = 1.4$, $\beta = 5.33$, $Q = 12.5$; (*b*) $\gamma = 1.4$, $\beta = 8.53$, $Q = 12.5$; (*c*) $\gamma = 1.4$, $\beta = 5.33$, $Q = 22.8$. (*a'–c'*) Numerical results for an Arrhenius law with the same values of the parameters as (*a–c*) respectively and plotted in the same non-dimensional form by using l_{iCJ}.

D_-. The $D(R_s)$ curve has a C-shaped form with a critical radius R_c as presented in figure 2. This has some analogies with the results obtained by Zeldovich (1940) and developed later by others (see Gelfand, Frolov & Nettleton 1990) on quenching phenomena of planar detonations propagating in rough tubes. These semi-phenomenological analyses were developed in the framework of a planar model of detonations with volumetric source terms accounting for heat and momentum losses at the walls. Inspired by the pioneering analyses of Zeldovich (1940), we first present in §3.2 an analytical solution of (3.1 *a–c*) in the framework of a square-wave model yielding a nonlinear relation for $D(R_s)$. It is shown that for $R_s > R_c$, the velocity spectrum of quasi-steady detonations is unbounded but presents two extrema; one, D_+, being a local minimum and the other, D_-, a local maximum, with a forbidden band $[D_+, D_-]$. An analytical expression for the critical radius R_c below which no generalized CJ solution exists, is obtained and it is shown that R_c is located in the domain of validity of approximated equations (3.1) or (3.2) (large radii of curvature, $R_s \gg 1$). These results are also compared in §3.3 with numerical solutions of (3.1 *a–c*) for an Arrhenius law. They are used later on for the determination of a critical energy of the direct initiation of detonations.

3.2. *Square-wave model*

The square-wave model is defined in a phenomenological way in the following manner. The chemical reaction is assumed to proceed in two sequential steps. The heat is released during a reaction time τ_r after a time delay called the induction time τ_i. The square-wave model corresponds to the limit $\tau_r/\tau_i \to 0$, for which the reaction rate ω becomes singular, and the heat release is localized in a thin exothermic layer considered as a discontinuity following the shock wave at a reduced distance l_i defined as

$$l_i \equiv v_N \tau_i, \tag{3.3a}$$

where the dimensionless induction time τ_i is highly sensitive only to the temperature fluctuations of the Neumann state just behind the shock wave, δT_N. Let $\beta = E_a/T_{NCJ}$ be the large reduced activation energy $(\delta\tau_i/\tau_i)/(\delta T_N/T_N) = O(\beta)$, $\beta \gg 1$, then

$$l_i/l_{iCJ} = \exp\{-\beta(T_N - T_{NCJ})/T_{NCJ}\} \quad \text{valid for} \quad \beta \gg 1, \tag{3.3b}$$

where subscripts N and CJ denote the Neumann state and the planar CJ case respectively and where, by definition of the reference lengthscale used in (2.1*a–d*), $l_{iCJ} = O(1)$. As shown in the Appendix, (3.3*b*) may be obtained from an Arrhenius law at the leading order of an asymptotic expansion in the distinguished limit, $\beta \to +\infty$, $\beta(\gamma-1)^2/4\gamma^2 = O(1)$, $(\gamma-1)^2 Q > 1 \Leftrightarrow (\gamma-1) D_{CJ}^2 > 1$. Equation (3.3*b*) represents the minimal model of the detonation structure to include the essential phenomena as well as the right orders of magnitude. Such a singular model has defects when describing the stability and the intrinsic dynamics of a detonation front which develops on the short characteristic timescale τ_i (Erpenbeck 1962, 1963). But this model was proved to be very useful to describe critical conditions appearing in the quasi-steady mechanisms developing on timescales much longer than τ_i (He & Clavin 1992).

When attention is focused on the case $\beta \gg 1$ and $R_s = O(\beta)$, the curvature terms in the right-hand sides of (3.1*a*, *b*) are of the same order of magnitude as $1/\beta$ and the variations of the Neumann temperature are small, $\delta T_N/T_N = O(1/\beta)$. But strong nonlinear effects are included at the leading order of the expansion in the limit $\beta \to +\infty$ because, according to the high sensitivity to T_N in (3.3*b*), one has $(\delta\tau_i/\tau_i) = O(1)$ and $(\delta l_i/l_i) = O(1)$. In the square-wave model, the thickness of the exothermic zone is negligibly small and the curvature effects modify only the induction zone which does not consume the reactant, $y = 1$. The thin exothermic zone is described in the phase plane by the same equation (3.2*d*) as in the planar case, but with an initial condition $v^2 = v_N^2(D)$ at $y = 1$ which differs from the planar case owing to the curvature effects across the induction zone. As for the planar case, the marginal solutions of the square-wave model may be obtained directly from the conservation laws across the detonation structure without investigating the trajectories in the phase space. These conservation laws are readily obtained by a ξ-integration of (3.1*a–c*) across the detonation structure and may be written in a dimensionless form as

$$\rho_b v_b = D - D\Gamma_1, \tag{3.4a}$$

$$\rho_b v_b^2 + p_b = (D^2+1) - D^2\Gamma_2, \tag{3.4b}$$

$$[\gamma/(\gamma-1)]p_b/\rho_b + \tfrac{1}{2}v_b^2 = \gamma/(\gamma-1) + \tfrac{1}{2}D^2 + Q, \tag{3.4c}$$

where the subscript b denotes the burned gases state at $y = 0$. The source terms of (3.4*a*, *b*), are defined by

$$\Gamma_1 = \frac{1}{D}\frac{j}{R_s}\int_0^{l_i} \rho(D-v)\,\mathrm{d}\xi, \quad \Gamma_2 = \frac{1}{D^2}\frac{j}{R_s}\int_0^{l_i} \rho(D-v)v\,\mathrm{d}\xi \tag{3.5a, b}$$

and represent the curvature-induced modifications of mass and momentum fluxes across the detonation structure. They are small perturbation terms and when they are neglected (3.4*a–c*) reduce to the ordinary Hugoniot relations. Using $1/R_s = O(1/\beta)$, the leading order of Γ_1 and Γ_2 in the asymptotic limit $\beta \to \infty$ can be easily computed from (3.5*a*, *b*) with the square-wave model by using the Neumann values of the planar CJ solution for D, v and ρ:

$$\Gamma_1 = j(\rho_{NCJ}-1)\frac{l_i}{R_s} = O\left(\frac{1}{\beta}\right), \quad \Gamma_2 = j\left(1-\frac{1}{\rho_{NCJ}}\right)\frac{l_i}{R_s} = \frac{1}{\rho_{NCJ}}\Gamma_1, \tag{3.6a, b}$$

where the thickness of the induction zone is given by (3.3*b*) and may be expressed in terms of the modification of detonation velocity $(D-D_{CJ})/D_{CJ}$ by using the Hugoniot relation for the leading shock in the fresh mixture,

$$\frac{T_N - T_{NCJ}}{T_{NCJ}} = \frac{2}{1+D_{CJ}^{-2}\gamma/(\gamma-1)}\frac{D-D_{CJ}}{D_{CJ}} \approx 2\frac{D-D_{CJ}}{D_{CJ}},$$

where the last approximation is valid for a sufficiently strong shock wave $(\gamma-1)D_{CJ}^2 > 1$, yielding

$$\frac{l_i}{l_{iCJ}} \approx \exp\left\{-2\beta\frac{D-D_{CJ}}{D_{CJ}}\right\}. \tag{3.6c}$$

By noticing that, according to (3.6*a–c*)

$$\delta\Gamma_{1,2} \approx -\frac{\delta D}{D_{CJ}}(2\beta\Gamma_{1,2}) \tag{3.6d}$$

a variation of (3.4*a–c*) around the marginal solution, defined by an extremum condition $\delta D = 0$, confirms that such a solution is still determined by the same sonic condition in the burned gases as in the planar case: $v_b = c_b = (\gamma p_b/\rho_b)^{1/2}$. Then, introducing $v_b = (\gamma p_b/\rho_b)^{1/2}$ in (3.4*a–c*), a perturbative analysis around the planar CJ detonation yields the curvature-induced modification of the detonation velocity $(D-D_{CJ})$ as a linear function of $\Gamma_1 = O(1/\beta)$ and $\Gamma_1 = O(1/\beta)$:

$$\left\{-\frac{2}{\gamma^2}\frac{\gamma(\gamma+1)+(\gamma^2-1)Q}{1+D_{CJ}^2}+\frac{2}{D_{CJ}^2}\right\}\frac{(D-D_{CJ})}{D_{CJ}} = \left(1+\frac{1}{D_{CJ}^2}\right)\Gamma_1-\Gamma_2. \tag{3.7}$$

Then, nonlinear relations (3.6*a–c*) yield a nonlinear equation for the velocity D of the marginal detonations:

$$\left(2\beta\frac{D_{CJ}-D}{D_{CJ}}\right)\exp\left(-2\beta\frac{D_{CJ}-D}{D_{CJ}}\right) = \frac{8j}{1-\gamma^2}\left(\beta\frac{l_{iCJ}}{R_s}\right), \tag{3.8}$$

where the strong-detonations assumption $((\gamma-1)D_{CJ}^2 > 1)$ has been used for simplicity. Equation (3.8) yields a nonlinear velocity–radius relation, $D(R_s)$, valid in the distinguished limit $\beta\to\infty$, $\beta l_{iCJ}/(\gamma-1)R_s = O(1)$, $\beta(D_{CJ}-D)/D_{CJ} = O(1)$, corresponding to a relatively small curvature intensity. This result exhibits a critical radius R_c,

$$\frac{R_c}{l_{iCJ}} = \frac{8ej}{1-\gamma^{-2}}\beta, \tag{3.9a}$$

below which no solution exits, and a corresponding critical detonation velocity D_c given by

$$\frac{D_{CJ}-D_c}{D_{CJ}} = \frac{1}{2\beta}. \tag{3.9b}$$

For $R_s > R_c$, (3.8) yields two branches of solutions $D_+(R_s) > D_-(R_s)$. The physical one is the upper one which reaches CJ planar solution from below when $R_s\to\infty$, $D_+(R_s)\to D_{CJ}$. The second solution branch, $D_-(R_s)$, is not physical: in the limit $R_s\to\infty$ one gets $\beta(D_{CJ}-D)/D_{CJ}\to\infty$ which does not correspond to the domain of validity of (3.8), $\beta(D_{CJ}-D)/D_{CJ} = O(1)$. We will discuss later the nature of this second solution branch. For weak curvature effects, $\beta l_{iCJ}/R_s\to 0$, one gets the following linear relation for the upper branch:

$$(D_{CJ}-D_+)/D_{CJ} = [4\gamma^2/(\gamma^2-1)]j(l_{iCJ}/R_s), \tag{3.9c}$$

which corresponds to the result of Klein & Stewart (1993) in the particular case of a one-step first-order reaction governed by an Arrhenius law at the limit of an infinitely large activation energy. Finally, notice that the numerical factor in the right-hand side of (3.9*a*) which controls the numerical value of the critical radius, is a larger number $8ej/(1-\gamma^{-2}) \approx 90$ for $\gamma = 1.4$ and $j = 2$ (spherical detonation). Thus, for ordinary

values of the reduced activation energy based on the Neumann temperature, $\beta = E_a/T_{NCJ} = 5$ to 10, the critical radius is 300 to 1000 times larger than the detonation thickness while the corresponding relative modification of the detonation velocity (3.9*b*) is small, 10^{-1} to 5×10^{-2}. In conclusion, the origin of the large value of R_c/l_{iCJ} is clearly exhibited by the square-wave model.

3.3. *Solutions for an Arrhenius law*

It is instructive to investigate numerically the case of a regular reaction rate such as an Arrhenius law (2.1*g*) with a moderate reduced activation energy $\beta = E_a/T_{NCJ} = 5$, yielding trajectories in the phase space v^2, y whose topological structure is different from the singular square-wave model. The system of equations (3.2*a*, *b*) is numerically integrated with (2.1*g*) by a Runge–Kutta method for a given D with an initial condition at $y = 1$ prescribed by the Hugoniot relation in the fresh mixture. Guided by the results presented above, a shooting method is used to find the radius R_s corresponding to the marginal solution whose trajectory passes through the saddle point, $v = c$ and $\psi = 0$, in the phase space (see the discussion at the end of §3.1). For a sufficiently large activation energy, the D, R_s curve so-obtained presents a C-shaped form, as predicted by the simplified analysis developed above. These curves are presented in figure 2 for different values of the parameters, in a dimensionless form, $2\beta(D-D_{CJ})/D_{CJ}$ *vs.* $R_s/j\beta l_{iCJ}$, which is suitable for comparison with the analytical results of the square-wave mode as obtained from (3.6*a–c*) and (3.7). The agreement is quite satisfactory. For a given R_s larger than the critical value R_c there are two trajectories corresponding to two different marginal detonation velocities D_+ and D_-. As clearly shown in figure 1(*b*), the trajectories corresponding to intermediate velocities of detonation, $D_- < D < D_+$, are the only ones for which there is no solution because of the presence of a singular point $\mathrm{d}v^2/\mathrm{d}y = +\infty$ at $y \neq 0$ ($v = c$ and $\psi > 0$). Thus, there are two disconnected continuous ranges of detonation velocities, the upper one $(D_+, +\infty)$ with a lower bound D_+ (local minimum) and another one with an upper bound D_-. D_- decreases and D_+ increases when R_s increases. When R_s decreases, the two trajectories (in the phase space $v^2 - y$) of the marginal solutions (D_+, D_-) become closer and closer and collapse at $R_s = R_c$ (see figure 1*c*), in such a way that there is no more local extrema for $R_s < R_c$. Except for the marginal solutions (when they exist), the flow behind the leading shock is subsonic everywhere (relatively to the shock) and the shock velocity will be continuously decreased by a rarefaction wave developing in the burned gases. Thus, only the upper branch D_+ of marginal solutions (minimum velocity) is selected, the other branch of solutions (D_- local maximum velocity) cannot be selected from below by the rarefaction wave.

4. Direct initiation

4.1. *Initiation criterion*

Consider now the direct initiation of a detonation by an energy source. As discussed in the introduction, the initial condition of the problem may be represented by self-similar solutions of a strong adiabatic blast waves (1.1*a*) which are represented by typical D–R_s curves, 1, 2, 3 in figure 3 where the C-shaped curve of the marginal quasi-steady solutions is also plotted. For self-propagating spherical or cylindrical detonations followed by a rarefaction wave, the selection of the generalized CJ solution follows the same mechanism as in the planar case (see (ii) in §1, the middle of §3.1, and the end of §3.3). Only the upper branch D_+ of the C-shaped curve may attract the unsteady solutions originating from the initial blast wave. This D_+ branch is the only

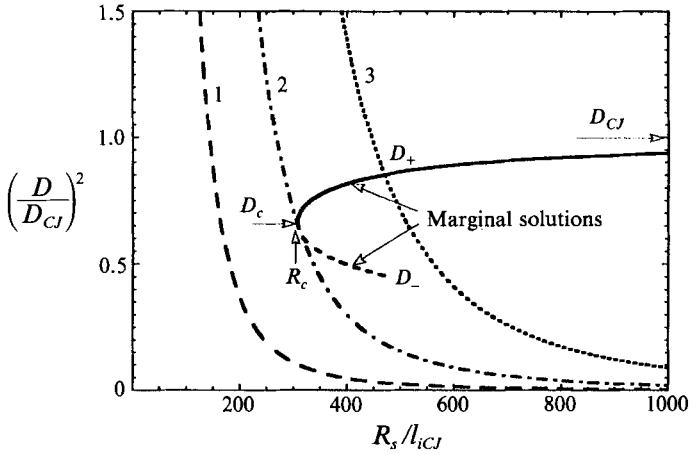

FIGURE 3. Schematic picture illustrating the criterion of detonation initiation governed by the nonlinear curvature effects. 1, 2, 3 are the D^2–R_s curves of the self-similar solutions (4.1) for strong adiabatic blast waves for three different values of the source energy. 1, $E_s < E_c$; 2, $E_s = E_c$; 3, $E_s > E_c$. The C-shaped curve of the marginal quasi-steady detonations is also plotted for comparison. Conditions of case 1 correspond to a subcritical case, and the initiation of a detonation is impossible. Cases 2 and 3 correspond roughly to critical and supercritical conditions for the successful initiation of detonation.

solution with a sonic point in the burned-gases region ($y \approx 0$) and corresponding to a minimum of the detonation velocity. Thus, as sketched in figure 3, ignition failures may be predicted for source energies E_s for which the D–R_s curve does not cross the upper branch D_+ (see case 1 in figure 3). Successful initiations may be expected in the opposite case (see case 3 in figure 3). As a result, an approximate critical energy $\tilde{E}_c$ may be obtained from (1.1a) by replacing $\tilde{R}_s$ by $\tilde{R}_c$ and $\tilde{D}$ by $\tilde{D}_c$,

$$\tilde{E}_c \approx k_j \tilde{\rho}_0 \tilde{R}_c^{j+1} \tilde{D}_c^2. \tag{4.1}$$

By using (3.9a, b), one obtains the following result:

$$\frac{E_c}{D_{CJ}^2 l_{iCJ}^{j+1}} \equiv \frac{\tilde{E}_c}{\tilde{\rho}_0 \tilde{D}_{CJ}^2 \tilde{l}_{CJ}^{j+1}} \approx k_j \left(\frac{8ej\beta}{1-1/\gamma^2}\right)^{j+1}. \tag{4.2}$$

The same result would be obtained by equating $\tilde{R}_c$ and $\tilde{R}^*(\tilde{E}_c)$ defined in §1. Equation (4.2), defining the critical energy, contains a huge factor $(\tilde{R}_c/\tilde{l}_{CJ})^{j+1} = (8ej\beta\gamma^2/(\gamma^2-1))^{j+1}$ with an order of magnitude between 10^7 and 10^9 in the spherical case. This shows that the critical radius and the critical energy are much larger than the detonation thickness $\tilde{l}_{CJ}$ and the energy $\tilde{\rho}_0 \tilde{D}_{CJ}^2 \tilde{l}_{CJ}^{j+1}$ (by unity of surface for $j = 0$, by unity of length for $j = 1$) involved in the Zeldovich *et al.* criterion (1956), respectively. The numerical simulations of a direct detonation initiation by an energy source, presented in the following subsection, confirm these theoretical predictions.

4.2. *Numerical results*

The time-dependent solutions of equations (2.1a–g) are obtained with a numerical code recently developed by He (1991) and He & Larrouturou (1994). The numerical method combines an upwind TVD shock-capturing method with a treatment of the shock wave and non-uniform gridding. This combination treats the shock as a real discontinuity and allows us to capture perfectly the Neumann spike. This numerical code has been proved to be very efficient in solving unsteady detonation problems with high precision such as quenching by thermal gradient (He & Clavin 1992).

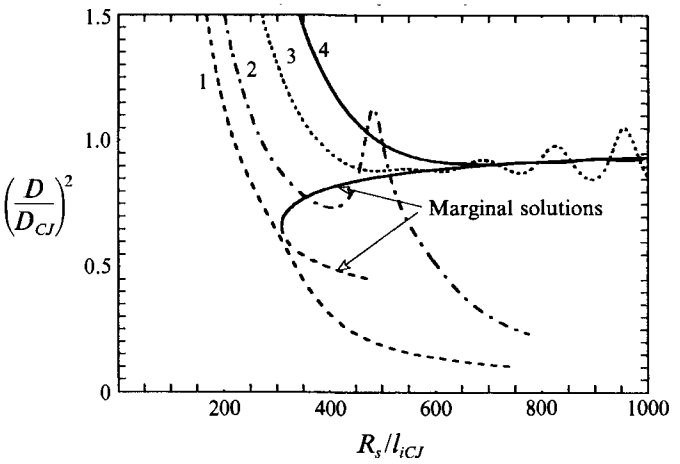

FIGURE 4. Numerical results of the initiation of spherical detonations. The front velocity is plotted as a function of the front radius and is compared with the corresponding marginal solutions for a reactive mixture characterized by $\gamma = 1.4$, $\beta = 5.33$, $Q = 12.5$ and for four values of the non-dimensional source energy $\tilde{E}_s/(\tilde{\rho}_0 \tilde{D}_{CJ}^2 \tilde{l}_{CJ}^3)$: 1, 3.30×10^7; 2, 5.69×10^7; 3, 1.34×10^8; 4, 2.64×10^8.

An amount of energy E_s is assumed to be released instantaneously (at constant volume) by the igniter in a uniform motionless reactive gas mixture at $t = 0$. The corresponding initial conditions are

$$\left.\begin{aligned} &p = p_s, \quad T = T_s, \quad y = 0, \quad u = 0, \qquad 0 \leqslant r < r_s, \\ &p_0 = T_0 = y_0 = 1, \quad u_0 = 0, \qquad r \geqslant r_s. \end{aligned}\right\} \tag{4.3a}$$

For $p_s \gg 1$, the released energy E_s (by unity of surface for $j = 0$, by unity of length for $j = 1$) is approximately

$$E_s \approx \sigma_j r_s^{j+1} p_s/(\gamma - 1) \quad \text{with} \quad \sigma_j = [2j\pi + (j-1)(j-2)]/(j+1). \tag{4.3b}$$

A very high initial pressure $p_s \approx 500$ (about 15 times larger than the peak pressure of the CJ detonation) and a small initial radius $r_s = 10$–80 (about 10 times smaller than the critical radius R_c) are used in such a way that a self-similar solution of the strong blast wave type (1.1) is developed at the early stages of the calculation.

The first calculations are performed for different values of the source energy E_s in spherical geometry with a set of parameters ($\gamma = 1.4$, $Q = 12.5$ and $E_a = 25 \Leftrightarrow \beta = 5.33$) for which the planar CJ detonation wave is stable. The velocity of the leading shock wave so obtained is plotted in figure 4 as a function of the radius of the front for four different source energies:

$$\tilde{E}_s/(\tilde{\rho}_0 \tilde{D}_{CJ}^2 \tilde{l}_{CJ}^3) = 3.30 \times 10^7,\ 5.69 \times 10^7,\ 1.34 \times 10^8 \quad \text{and} \quad 2.64 \times 10^8.$$

The C-shaped curve representing the quasi-steady marginal detonations described in §3.3 is also plotted in the same figure.

Case 1, which is associated with the lowest source energy, $\tilde{E}_s/(\tilde{\rho}_0 \tilde{D}_{CJ}^2 \tilde{l}_{CJ}^3) = 3.30 \times 10^7$, corresponds to a slightly subcritical case leading to a failure of the detonation initiation. The velocity of the leading shock becomes smaller than the critical velocity D_c before reaching the critical radius R_c. At $R_s/l_{iCJ} = 700$, this velocity is about $D^2/D_{CJ}^2 = 0.2$ and the temperature in the reactive mixture compressed by the shock is too low to produce a rapid ignition, the chemical reaction front decouples from the leading shock. Failures occur for all cases with an initiation energy smaller

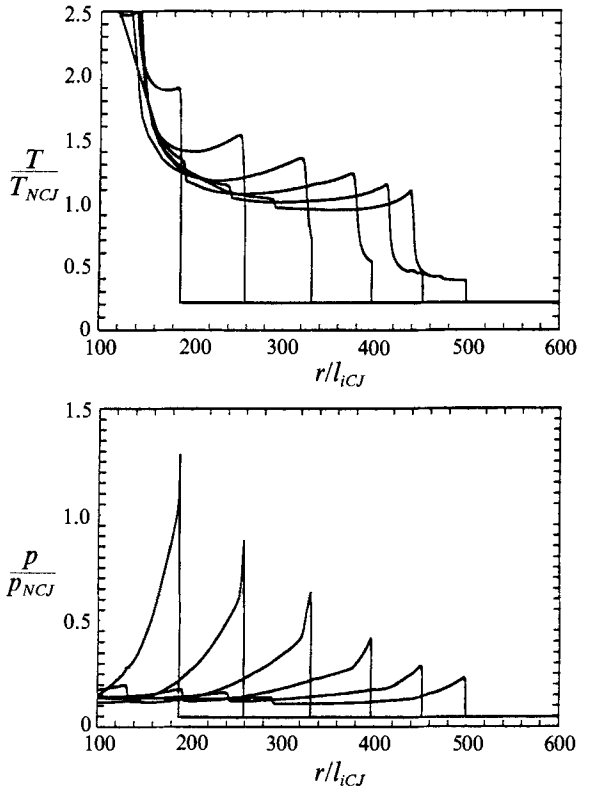

FIGURE 5. Temperature and pressure profiles at different instants in time for case 1 of figure 4, corresponding to an ignition failure.

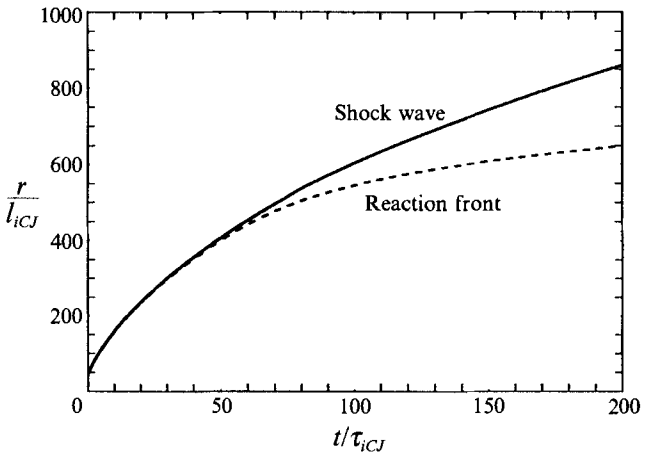

FIGURE 6. Shock wave and reaction front-trajectories for case 1 of figure 4; the position of the reaction front is defined as $y = 0.5$.

than that of case 1. Typical profiles for pressure and temperature characterizing the detonation structure just below the critical radius are shown in figure 5 and the exothermic reaction region and shock trajectories are shown on an r–t diagram in figure 6.

Case 4, which is associated with the strongest source energy, $\tilde{E}_s/(\tilde{\rho}_0 \tilde{D}_{CJ}^2 \tilde{l}_{CJ}^3) =$

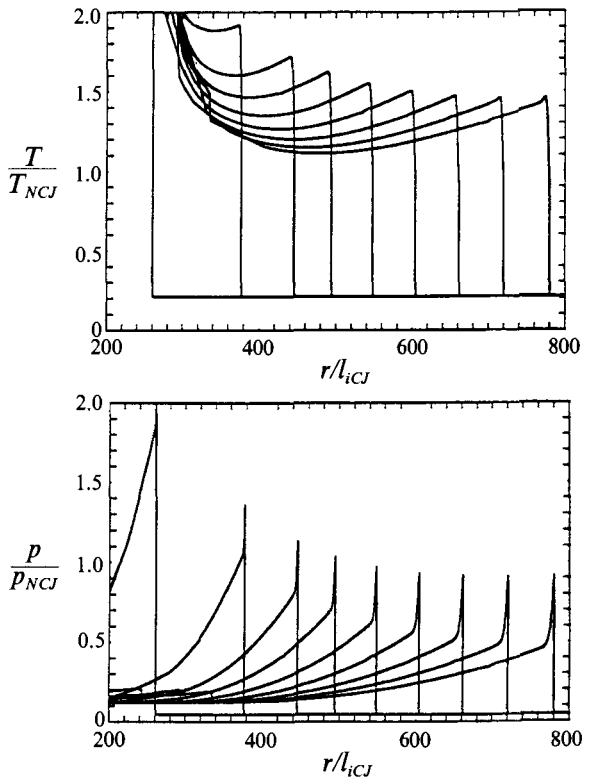

FIGURE 7. Temperature and pressure profiles at different instants in time for case 4 of figure 4, corresponding to a successful initiation of a CJ detonation.

2.64×10^8, corresponds to a successful initiation of the detonation. The upper branch of marginal quasi-steady solutions of (3.2*a–c*) quickly attracts the unsteady blast wave. At about $R_s/l_{iCJ} = 700$ this quasi-steady regime is reached and the numerical solution follows closely the D_+ solution at later times. This upper branch, corresponding to a generalized CJ detonation, plays the role of an attractor for the initial blast waves and represents with a good accuracy the self-sustained expanding detonations. Typical profiles are presented in figure 7.

Case 3, with an intermediate source energy $\tilde{E}_s/(\tilde{\rho}_0 \tilde{D}_{CJ}^2 \tilde{l}_{CJ}^3) = 1.34 \times 10^8$, shows a successful initiation but presenting unsteady effects on a short timescale ($\approx 10\tau_{iCJ}$) characterizing the response of the detonation structure. When the trajectory reaches the upper D_+ branch, galloping oscillations first develop and finally die out later on (see figure 8). This shows that, even for a stable planar detonation wave, the first part of the upper D_+ branch is unstable in a neighbourhood of the critical condition ($R_s = R_c$). According to the numerical results presented in figure 8, the stability limit is about $R_s/l_{iCJ} = 1200$. This one-dimensional detonation instability mechanism is similar to the one which is known to appear in the planar case at a sufficiently large reduced activation energy E_a/T_N. Let us denote by β_c the corresponding critical value of E_a/T_N. The stability limit of the D_+ branch may be estimated from that obtained numerically in the planar case (Erpenbeck 1962; Lee & Stewart 1990): as a result of the front curvature, the decrease of the Neumann temperature T_N produces an increase of E_a/T_N yielding the instability shown in figure 8, occurring when $\beta > \beta_c$. Case 4 is similar to case 3 shown in figure 8, but with a negligible maximum amplitude of oscillation.

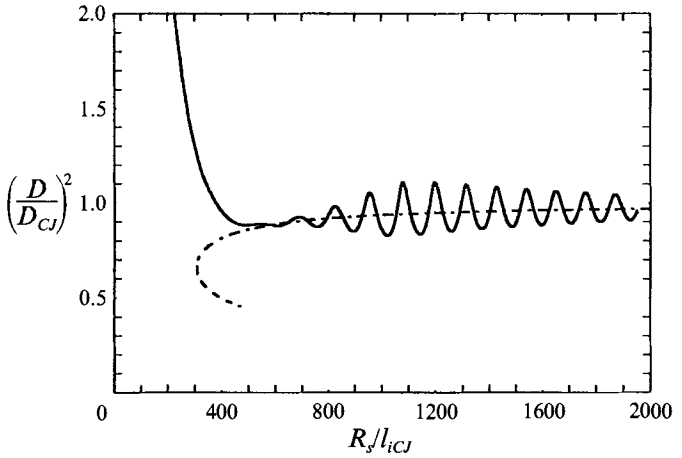

FIGURE 8. Detonation velocity as a function of the front radius for case 3 of figure 4 (stable planar CJ detonation) illustrating the linear growth and the final damping of the oscillating instability.

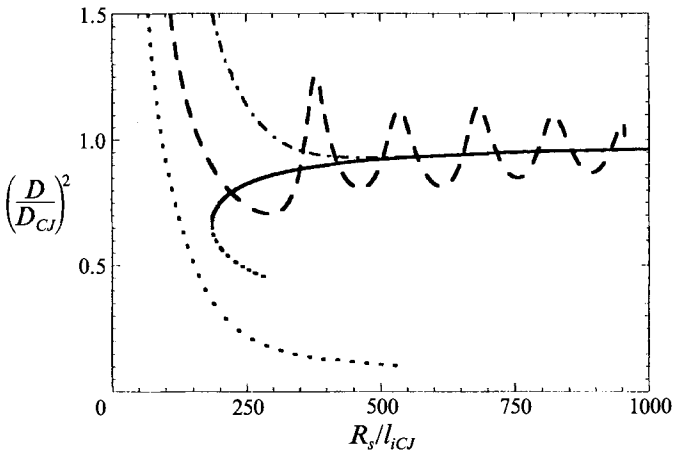

FIGURE 9. Numerical results for the direct initiation of a cylindrical detonation for a reactive mixture characterized by $\gamma = 1.4$, $\beta = 5.33$, $Q = 12.5$ and three values of the non-dimensional source energy per unit length $\tilde{E}_s/(\tilde{\rho}_0 \tilde{D}_{CJ}^2 \tilde{l}_{CJ}^2)$: 1, 1.33×10^4; 2, 3.40×10^4; 3, 5.33×10^4.

When the source energy E_s decreases, the contact point between the trajectory of the initial blast wave and the D_+ branch approaches the critical point. The maximum oscillation amplitude of the galloping oscillations increases and may lead to a failure of the detonation initiation even for E_s slightly larger than the critical value $\tilde{E}_c/(\tilde{\rho}_0 \tilde{D}_{CJ}^2 \tilde{l}_{CJ}^3) \approx 3.5 \times 10^7$. This is illustrated by case 2 shown in figure 4 with $\tilde{E}_s/(\tilde{\rho}_0 \tilde{D}_{CJ}^2 \tilde{l}_{CJ}^3) = 5.68 \times 10^7$.

The initiation problem is very similar for ranges of parameters (γ, Q, E_a) corresponding to weakly unstable planar detonation fronts. As explained in the following section, the case of very unstable planar fronts (very large reduced activation energies) remains open. Results for cylindrical geometry like the ones presented in figure 9, are qualitatively similar to those for the spherical geometry.

5. Discussion of the results

The results presented in this paper show clearly that the criterion for a direct detonation initiation by an energy source in cylindrical and spherical geometry is directly controlled by nonlinear curvature effects of the detonation front, at least in the range of parameters where the planar detonation is not strongly unstable.

The order of magnitude of the critical radius $\tilde{R}_c$ (3.9*a*), as obtained analytically with the square-wave model, is 300 to 1000 times larger than the induction length $\tilde{l}_{CJ}$ (see the end of §3.2), which is in good agreement with the direct numerical simulations of detonations initiation reported in §4.2. This order of magnitude is also in agreement with the experiments of Desbordes (1986) reported in introduction. Concerning the critical energy $\tilde{E}_c$, the order of magnitude predicted by (4.2) is in agreement with both the direct numerical simulations and the phenomenological expressions which yield the best fit with the experimental data like (5) of Lee (1984). This last expression is based on the experimental correlation $\tilde{R}_c = 13\lambda/4$, where λ is the cell size. As an example, (4.2) yields $\tilde{E}_c/(\tilde{\rho}_0 \tilde{D}_{CJ}^2 \tilde{l}_{CJ}^3) = 4.45 \times 10^8$ (spherical case) and $\tilde{E}_c/(\tilde{\rho}_0 \tilde{D}_{CJ}^2 \tilde{l}_{CJ}^2) = 1.87 \times 10^5$ (cylindrical case) for the same conditions as in figures 4 and 9 respectively, values which are less than ten times larger than the numerical results. A similar ratio is obtained for the spherical case when (4.2) is compared with the above-mentioned formula of Lee and by using his correlation between the cell size and the induction length $\lambda \approx 50\tilde{l}_{CJ}$ valid for hydrogen–air mixtures (Lee 1984).

The critical radius and energy as predicted by (3.9*a*) and (4.2) are much larger than $\tilde{l}_{CJ}$ and $\tilde{\rho}_0 \tilde{D}_{CJ}^2 \tilde{l}_{CJ}^{j+1}$ (the criterion of Zeldovich *et al.* 1956), essentially because of the very large non-dimensional parameter, $8ej\beta\gamma^2/(\gamma^2-1) \approx 300$ to 1000, measuring the high sensitivity of the detonation structure to the Neumann temperature. As a result of this high sensitivity, a small curvature of the detonation front, $\tilde{l}_{CJ}/\tilde{R}_s \ll 1$, produces a strong effect and the detonation velocity is close to its planar CJ value even at the critical condition.

The approximate character of these theoretical results is due essentially to four factors: (i) unsteady effects illustrated by case 2 in figure 4 are not considered; (ii) multidimensional effects yielding cellular detonation fronts are also neglected; (iii) the critical condition is obtained in an asymptotic limit corresponding to the square-wave model; (iv) the strong non-reactive blast waves approximation (4.1) is used for the initial decay of the reactive blast wave.

When considering the unsteady effects, one must first discuss the validity of the quasi-steady-state approximation used in (3.1*a–d*) to determine the D_+ branch of solutions acting as an attractor. The characteristic evolution rate of the D_+ branch solutions, $1/t_e \equiv \mathrm{d}D_+/\mathrm{d}R_s$, is given far enough from the critical point by (3.9*c*), yielding $1/t_e = 4j\gamma^2(\gamma^2-1)^{-1}(l_{iCJ}/R_s)^2(D_{CJ}/l_{iCJ})$. This shows that, when $l_{iCJ}/R_s = O(1/\beta)$, the unsteady terms $\partial/\partial\tau$ neglected in (3.1*a–d*) are effectively of the following order in the large-radius expansion: $\tau_{iCJ}/t_e = O(\beta^{-2})$. This approximation does not hold close to the critical point where $\mathrm{d}D_+/\mathrm{d}R_s \to \infty$ but this does not change the final results because this divergence affects only a small vicinity of the critical point.

The quasi-steady state is obviously not valid to represent the unsteady effects related to the intrinsic dynamical properties of the marginal solution D_+ involving a characteristic timescale of same order of magnitude as $\tilde{t}_{CJ}$. The CJ planar detonation is known to become unstable for a sufficiently high activation energy. As discussed for cases 3 and 4 in §4.2 ($\beta = 5.3$), the instability mechanism is reinforced when approaching the critical point. For a larger activation energy, stronger unsteady effects are observed, as in figure 10 ($\beta = 6.4$) corresponding to an unstable planar CJ

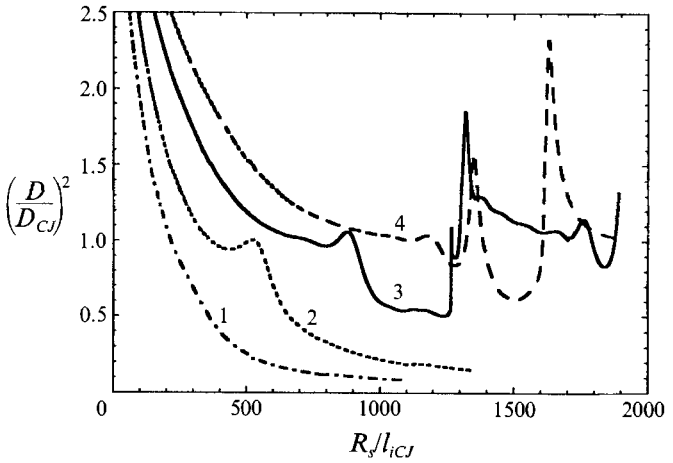

FIGURE 10. Numerical results for the direct initiation of a cylindrical detonation for a reactive mixture characterized by $\gamma = 1.2$, $\beta = 6.4$, $Q = 50$ and four values of the non-dimensional source energy per unit length $\tilde{E}_s/(\tilde{\rho}_0 \tilde{D}_{CJ}^2 \tilde{l}_{CJ}^2)$: 1, 7.34×10^4; 2, 1.66×10^5; 3, 4.61×10^5; 4, 1.71×10^6.

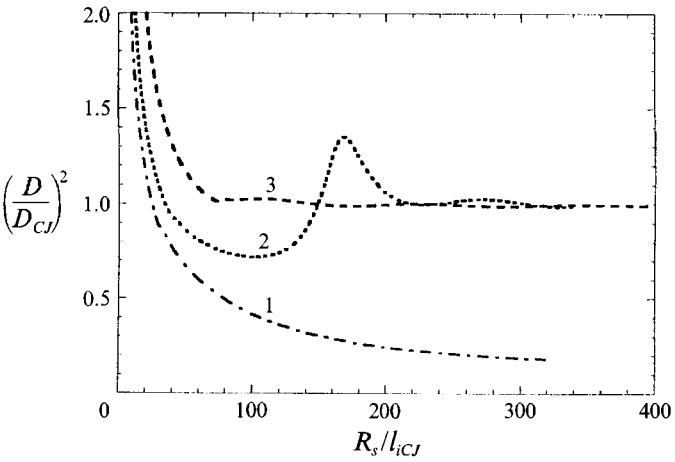

FIGURE 11. Numerical results for the direct initiation of a planar detonation for a reactive mixture characterized by $\gamma = 1.4$, $\beta = 5.33$, $Q = 12.5$ and three values of the non-dimensional source energy per unit surface $\tilde{E}_s/(\tilde{\rho}_0 \tilde{D}_{CJ}^2 \tilde{l}_{CJ})$: 1, 28.1; 2, 34.1; 3, 51.87.

detonation. The critical radius is $\tilde{R}_c/\tilde{l}_{CJ} \approx 500$ and curve 3 of figure 10 exhibits a detonation quenching followed by a sudden re-ignition. Such phenomena have been observed experimentally (see for example Desbordes 1986). Thus, the intrinsic dynamics cannot always be ignored in the detonation ignition, especially for strongly unstable detonations.

Strong unsteady effects are obviously always present during the first stage of ignition but they do not necessarily control the critical conditions. This is demonstrated by comparison with numerical studies in planar geometry where the curvature effects are absent. The results in figure 11 correspond to the same set of parameters as in figures 4–9. The critical size is forty times larger than the detonation thickness but it is ten times smaller than the critical radius in spherical geometry. This shows that the quasi-steady curvature effects are dominant in spherical and cylindrical geometries for determining the ignition condition of stable detonations.

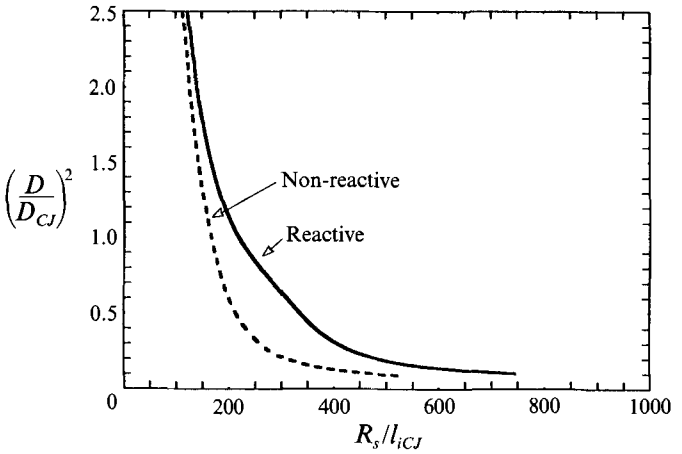

FIGURE 12. Comparison between the decay of the inert and reactive blast waves at the critical condition (case 1 of figure 4).

Multidimensional effects remain an open question. Cells develop when the smooth detonation front loses its stability. In figures 4–9, the linear instability growth rate is small enough that developments of cells are not expected to modify the initiation criterion. The case of strongly unstable detonations is less clear.

The square-wave model has been known for a long time to be pathological for the intrinsic dynamics of detonation fronts (Erpenbeck 1963). Corresponding to an infinite activation energy, it leads to a non-physical spectrum of unbounded growth rates with unbounded oscillation frequencies. But it was proved to be a good candidate to describe analytically the quasi-steady phenomena of detonations associated with a high temperature sensitivity (He & Clavin 1992).

Finally, as shown by a comparison of the two trajectories of the reactive and non-reactive blast waves with the same critical energy (figure 12), the use of self-similar solutions of adiabatic blast waves (1.1*a*) with (3.9*a*, *b*) to determine the critical condition (4.2), corresponds to a fairly good approximation for the order of magnitude of the critical parameters.

We thank Professor Amable Liñan and Doctor Guy Joulin for fruitful discussions.

Appendix

The conservation equation (3.1*c*) of the total enthalpy (2.5) yields

$$\frac{\mathrm{d}T}{\mathrm{d}\xi} = -\frac{\gamma-1}{\gamma}\left(v\frac{\mathrm{d}v}{\mathrm{d}\xi}+Q\frac{\mathrm{d}y}{\mathrm{d}\xi}\right). \tag{A 1}$$

Using (3.2*a*) and (3.1*d*), one obtains the following equation for the temperature distribution:

$$v\frac{\mathrm{d}T}{\mathrm{d}\xi} = \frac{c^2-\gamma v^2(\gamma-1)Q}{c^2-v^2}\frac{}{\gamma}\tilde{B}\tilde{t}_{ref}\,y\exp\left(-\frac{E_a}{T}\right)+\frac{\gamma-1}{\gamma}\frac{v^2}{c^2-v^2}\frac{j}{R_s}(D-v)c^2, \tag{A 2a}$$

$$v\frac{\mathrm{d}y}{\mathrm{d}\xi} = -\tilde{B}\tilde{t}_{ref}\,y\exp\left(-\frac{E_a}{T}\right). \tag{A 2b}$$

When $\beta \equiv E_a/T_N \gg 1$, the temperature profile exhibits two lengthscales. The temperature variation is relatively weak, $\delta T/T_N = O(1/\beta)$ across an induction zone of reduced thickness l_i at the end of which the temperature varies strongly $\delta T/T_N = O(1/\gamma - 1)$ within a thin exothermic zone, $\delta\xi/l_i = O(1/\beta)$. In the induction zone one has

$$\frac{T}{T_N} = 1 + \frac{1}{\beta}\Theta + O\left(\frac{1}{\beta^2}\right), \quad \frac{v}{v_N} = 1 + O\left(\frac{1}{\beta}\right), \tag{A 3}$$

where $\Theta = O(1)$. The leading order of the reduced induction length l_i is determined by the runaway of Θ which is given by the following equation for a Mach number $M_N \equiv v_N/c_N$ smaller than $1/\gamma^{1/2}$:

$$\frac{\mathrm{d}\Theta}{\mathrm{d}\xi} = \frac{1-\gamma M_N^2}{1-M_N^2}\frac{1}{v_N}\frac{\mathrm{e}^{E_a/T_{NCJ}}}{\mathrm{e}^{E_a/T_N}} y\,\mathrm{e}^{\Theta} + (\gamma-1)\frac{M_N^2}{1-M_N^2}\left(\frac{D}{v_N}-1\right)\beta\frac{j}{R_s}. \tag{A 4}$$

Equation (A 4) is obtained in a straightforward manner from (A 2) by introducing expansions (A 3) and definition (2.2). The assumption $M_N < 1/\gamma^{1/2}$ is valid for sufficiently strong shock waves like those involved in detonations. Then, by introducing the dimensionless lengthscale l_i defined as

$$l_i \equiv \frac{1-M_N^2}{1-\gamma M_N^2} v_N\,\mathrm{e}^{E_a/T_N - E_a/T_{NCJ}} \tag{A 5}$$

and the dimensionless variable $x = \xi/l_i$ ($\mathrm{d}x/\mathrm{d}\xi > 0$), (A 4$a$, b) takes the following simplified form:

$$\frac{\mathrm{d}\Theta}{\mathrm{d}x} = y\,\mathrm{e}^{\Theta} + a, \quad \frac{\mathrm{d}y}{\mathrm{d}x} = -\frac{1}{\beta} b y\,\mathrm{e}^{\Theta}, \tag{A 6a, b}$$

where the non-dimensional parameters a and b characterize the curvature effect and the inverse of the heat release respectively,

$$a \equiv (\gamma-1)\frac{M_N^2}{1-M_N^2}\left(\frac{D}{v_N}-1\right)j\beta\frac{l_i}{R_s}, \quad b \equiv \frac{1-M_N^2}{1-\gamma M_N^2}\frac{\gamma}{\gamma-1}\frac{T_N}{Q}. \tag{A 7a, b}$$

If $$b = O(1) \quad \text{or} \quad b = o(1) \quad \text{when} \quad \beta \to \infty, \tag{A 8a}$$

one has, according to (A 6b), $y \approx 1$ valid in all the induction zone. Then, at the leading order of the asymptotic expansion, (A 6a) reduces to $\mathrm{d}\Theta/\mathrm{d}x = \exp(\Theta) + a$, whose solution satisfying the initial condition $\Theta = 0$ at $x = 0$ is

$$\Theta = ax - \ln\left(1 - \frac{\mathrm{e}^{ax}-1}{a}\right). \tag{A 8b}$$

The parameter x_i characterizing the induction length is defined by the runaway of Θ,

$$\Theta \to \infty \quad \text{when} \quad x \to x_i,$$

and (A 8b) yields

$$x_i \equiv \frac{1}{a}\ln(1+a). \tag{A 8}$$

In the limit of a small curvature effect, $a \to 0 \Rightarrow x_i \to 1$, the dimensionless induction length is given by (A 5) and thus (3.3b) is verified. This corresponds to the following

dimensional forms for the induction time $\tilde{t}_{CJ}$ and the induction length l_{CJ} of the planar CJ detonation:

$$\tilde{t}_{CJ} = \tau_{iCJ}\,\tilde{t}_{ref} \quad \text{with} \quad \tau_{iCJ} \equiv \frac{1-M_{NCJ}^2}{1-\gamma M_{NCJ}^2}, \tag{A 9a}$$

$$\tilde{l}_{CJ} = l_{iCJ}\,\tilde{r}_{ref} \quad \text{with} \quad l_{iCJ} = \tau_{iCJ}\,v_{NCJ}, \tag{A 9b}$$

where the reference time- and lengthscales $\tilde{t}_{ref}$ and $\tilde{r}_{ref}$ are defined in §2 in such a way that the reduced induction time and length are of order unity, $\tau_{iCJ} = O(1)$ and $l_{iCJ} = O(1)$ when $\beta \to \infty$. Notice that according to (A 8*c*), one has $x_i = 1 + O(1/\beta)$ when $a = O(1/\beta)$.

In the approximation of a strong shock

$$(\gamma-1)\,D^2 > 1 \tag{A 10a}$$

the Hugoniot relations yields

$$\frac{M_N^2}{1-M_N^2}\left(\frac{D}{v_N}-1\right) \approx \frac{2}{\gamma+1} \tag{A 10b}$$

and the relations for CJ detonations lead to

$$D_{CJ}^2 \approx 2(\gamma+1)(\gamma-1)\,Q \quad \text{and} \quad \frac{T_{NCJ}}{(\gamma-1)\,Q} \approx 4\frac{\gamma-1}{\gamma+1}. \tag{A 10c}$$

Then the distinguished limit

$$\beta \to \infty, \quad (\gamma-1) = O(1/\beta), \quad (\gamma-1)\,D^2 > 1, \quad (l_i/R_s) = O(1/\beta), \tag{A 11}$$

yields $a = O(1/\beta)$ and $b = O(1/\beta)$ and the leading order of the induction length is given by (A 5).

The value of the curvature parameter at the critical radius $a = a_c$ is obtained by anticipating result (3.9*a*) to give

$$a_c = (\gamma-1)^2/4\gamma^2. \tag{A 12}$$

This is a very small number indeed ($a_c \approx 7\times10^{-3}$ and 2×10^{-2} for $\gamma = 1.2$ and 1.4 respectively) yielding, according to (A 8*c*), a negligible correction to $x_i = 1$. The relevant curvature effect is fully included in (A 5) through the modification of the Neumann temperature T_N. From the point of view of the asymptotic expansion, (A 12) shows that the validity of model (A 5) and (3.3*b*) for describing the upper branch D_+ of curved detonation fronts, is extended to the assumption $\beta(\gamma-1)^2/4\gamma^2 = O(1) \Rightarrow a_c = O(1/\beta)$. This is an even less restrictive assumption than (A 11) and is well verified for all gaseous mixtures.

REFERENCES

BARENBLATT, G. I., GUIRGUIS, R. H., KAMEL, M. M., KUHL, A. L., OPPENHEIM, A. K. & ZELDOVICH, YA. B. 1980 Self-similar explosion waves of variable energy at the front. *J. Fluid Mech.* **99**, 841–859.

BDZIL, J. B. 1981 Steady-state two-dimensional detonation. *J. Fluid Mech.* **108**, 195–226.

DESBORDES, D. 1986 Correlations between shock flame predetonation zone size and cell spacing in critically initiated spherical detonations. *Prog. Astronaut. Aeronaut.* **106**, 166.

ERPENBECK, J. J. 1962 Stability of steady-state equilibrium detonations. *Phys. Fluids* **5**, 604–614.

ERPENBECK, J. J. 1963 Structure and stability of the square-wave detonation. In *9th Symp. (Intl) on Combustion*, pp. 442–453. Academic.

FICKETT, N. & DAVIS, W. C. 1979 *Detonation*. University of California Press, Berkeley.

GELFAND, B. E., FROLOV, S. M. & NETTLETON, M. A. 1991 Gaseous detonations – A selected review. *Prog. Energy Combust. Sci.* **17**, 327.

HE, L. T. 1991 A study of the ignition phenomena. Applications to H_2/O_2 mixtures. Thèse de l'Université d'Aix-Marseille I (France).

HE, L. T. & CLAVIN, P. 1992 Critical conditions for detonation initiation in cold gaseous mixtures by nonuniform hot pockets of reactive gases. In *24th Symp. (Intl) on Combustion*, pp. 1861–1867. The Combustion Institute.

HE, L. T. & CLAVIN, P. 1993 Premixed hydrogen-oxygen flames. Part I: and Part II Flame structure and quasi-isobaric ignition near the flammability limits. *Combust. Flame* **93**, 391–420.

HE, L. T. & LARROUTUROU, B. 1994 Moving grid numerical simulations of planar time-dependent detonations. *J. Comput. Phys.* (submitted).

JOULIN, G. & CLAVIN, P. 1976 Analyse asymptotique des conditions d'extinction des flammes laminaires. *Acta Astronautica* **3**, 223–240.

KLEIN, R. & STEWART, D. S. 1993 The influence of the reaction rate – state dependence on the curvature-detonation speed relation. *SIAM J. Appl. Maths* **54**, 1401.

KOROBEINIKOV, V. P. 1971 Gas dynamics of explosions. *Ann. Rev. Fluid Mech.* **3**, 317–346.

LAFFITTE, P. 1925 Recherches experimentales sur l'onde explosive et l'onde de choc. *Ann. Phys.* **10**, 623–634.

LANDAU, L. & LIFCHITZ, E. 1989 *Mecanique des Fluids*, 2nd Edn. MIR.

LEE, H. I. & STEWART, D. S. 1990 Calculation of linear detonation instability: one-dimensional instability of plane detonations. *J. Fluid Mech.* **216**, 103.

LEE, J. H. 1977 Initiation of gaseous detonation. *Ann. Rev. Phys. Chem.* **28**, 75–104.

LEE, J. H. 1984 Dynamic parameters of gaseous detonations. *Ann. Rev. Fluid Mech.* **16**, 311–336.

LIÑAN, A. 1974 The asymptotic structure of counter flow diffusion flames for large activation energies. *Acta Astronautica* **1**, 1007–1039.

SEDOV, L. I. 1946 Propagation of strong blast waves. *Prikl. Mat. Mech.* **10**, 241–250.

TAYLOR, G. I. 1950*a* The dynamics of the combustion products behind plane and spherical detonation front in explosives. *Proc. R. Soc. Lond.* A **200**, 235–247.

TAYLOR, G. I. 1950*b* The formation of a blast wave by a very intense explosion I. Theoretical discussion. *Proc. R. Soc. Lond* A **201**, 159–174.

ZELDOVICH, YA. B. 1940 On the theory of detonation propagation in gaseous systems. In *Selected Works of Yakov Borisvich Zeldovich, Volume I Chemical Physics and Hydrodynamics* (ed. J. P. Ostriker, G. I. Barenblatt & R. A. Sunyaev), 1992, pp. 411–451. Princeton University Press.

ZELDOVICH, YA. B. 1942 Distribution of pressure and velocity in the products of a detonation explosion, and in particular in the case of a spherical propagation of the detonation waves. *J. Exp. Theor. Phys.* (USSR) **12**, 389–406.

ZELDOVICH, YA. B., KOGARKO, S. M. & SIMONOV, N. N. 1956 An experimental investigation of spherical detonation of gases. *Sov. Phys. Tech. Phys.* **1** (8), 1689–1731.